JAERI-M
7043

JFT-2 TOKAMAK NEUTRAL INJECTOR AND PRELIMINARY RESULTS OF ADDITIONAL HEATING EXPERIMENT

April 1977

T. SUGAWARA[*1], M. AKIBA[*2], Y. ARAKAWA[*3], N. FUJISAWA,
A. FUNAHASHI, T. HIRAYAMA, H. HORIIKE[*4], T. ITOH,
U. KONDOH[*5], S. KONOSHIMA, M.MAENO, S. MATSUDA,
Y. OHARA, T. OHGA, T. SHIBATA, M. SHIMADA,
H. SHIRAKATA, N. SUZUKI, K. TAKAHASHI,
H. TAKEUCHI, S. TANAKA and T. YAMAMOTO[*6]

日本原子力研究所
Japan Atomic Energy Research Institute

JFT-2 Tokamak Neutral Injector and Preliminary results of Additional Heating Experiment

Tohru SUGAWARA[*1], Mitsunori AKIBA[*2], Yoshihiro ARAKAWA[*3], Noboru FUJISAWA, Akimasa FUNAHASHI, Toshio HIRAYAMA, Hiroshi HORIIKE[*4], Takao ITOH, Umeo KONDOH[*5], Shigeru KONOSHIMA, Masaki MAENO, Shinzaburo MATSUDA, Yoshihiro OHARA, Tokumichi OHGA, Takemasa SHIBATA, Michiya SHIMADA, Hirofumi SHIRAKATA, Norio SUZUKI, Kohki TAKAHASHI, Hiroshi TAKEUCHI, Shigeru TANAKA and Takumi YAMAMOTO[*6].

Division of Thermonuclear Fusion Research, Tokai, JAERI

(Received March 24, 1977)

A nearly perpendicular injection system of two beam lines for JFT-2 tokamak device is described. Ion heating is obtained up to about 15 % rise of target ion temperature using the system. Its heating efficiency is in agreement with the empirical scaling law.

---

*1) On leave from Research and Development Center, Tokyo Shibaura Electric Co., Ltd.

*2) On leave from Tokyo Institute of Technologiy.

*3) On leave from University of Tokyo.

*4) On leave from Osaka University.

*5) On leave from Nissin Electric Co., Ltd.

*6) On leave from Nagoya University.

JFT－2用中性粒子入射装置と加熱の初期実験結果

日本原子力研究所東海研究所核融合研究部

菅原　亨[*1]・秋葉　光徳[*2]・荒川　義博[*3]・藤沢　登・船橋　昭昌
平山　俊雄・堀池　寛[*4]・伊藤　孝雄・近藤　梅夫[*5]・木島　滋
前野　勝樹・松田慎三郎・小原　祥裕・大賀　徳道・柴田　猛順
嶋田　道也・白形　弘文・鈴木　紀男・高橋　興起・竹内　浩
田中　茂・山本　巧[*6]

（1977年3月24日受理）

JFT－2トカマクに取付けられた中性粒子入射装置の構成と，本装置による加熱実験の初期結果について述べられている。この入射装置は，二つのビーム・ラインから成り，ビームは，プラズマ電流にほぼ垂直に打込まれた。本装置を用いて，約15％のイオン温度上昇を達成した。この温度上昇は，経験則に合致しており，古典論に基づいて説明しうることが示された。

＊1　外来研究員　東芝総合研究所
＊2　特別研究生　東京工業大学
＊3　特別研究生　東京大学
＊4　特別研究生　大阪大学
＊5　外来研究員　日新電機
＊6　特別研究生　名古屋大学

目　次　な　し

§1 Introduction

Neutral beam injection heating of JFT-2 tokamak plasma is made in order to study the techniques and physics of beam heating. The injection system was completed in the end of the first half year of 1976. Immediately afterwards, the additional heating experiment started. The power level absorbed by a target plasma is low as compared with those of TFR[1] and ORMAK[2]. As a result, the ion temperature rise was relatively small. However, the rise was obtained up to about 15% of target ion temperature. The present report gives an outline of injection system and some preliminary results on a heating study.

Injection is made at an angle of 85 degrees to the plasma current under the constraints of JFT-2 device. In the next section, a brief description of the design considerations and characteristics of the system is presented. Ion heating is studied under the ion source drain current of 6 A at 30 kV and 8 A at 25 kV in total. Section 3 describes the experimental procedure and the results, together with the discussion based on the classical theory.

§2 Neutral Beam Injector

A tangential injection is desirable for efficient trapping of the neutral beam. For tangential injection, however, the large-scale alternation of JFT-2 device such as the reconstruction of toroidal coils and tangential port cannot be avoided. It is a problem to accompany the alternation that the shut-down period is extended. Therefore the injection angle was chosen to be 85-95 degrees to the plasma current, and JFT-2 device is not altered except for installation of beam dumper in the vacuum chamber. The whole aspect of injector is illustrated in Fig. 1. Two beam lines are located at 20 degrees with respect to the median plane and are focalized at the axis of JFT-2 vacuum vessel.

The line includes the ion source(1), neutralizer(2), magnetic shield(3), flashing target(4), drift tube(5), titanium sublimer(6), molybdenum target(7) and isolation valves. The distance between the ion source and injection window is 1.35 m. The window is of 56 mm x 120 mm, and is restricted by the gap between toroidal coils.

Two ion sources are of duoPIGatron[3] as shown in Fig. 2. The accel-decel grids of 7 cm in diameter have 225 recessed apertures of 3.75 mm diameter each. The beamlets from multi-apertures are focalized using the aperture displacement method[4]. The designed focal length is 1.4 m. In addition, the electrode in contact with the source plasma is curved to match the radially decreased ion-saturation-current density of source with the extraction current density. Figure 3 gives the extraction electrodes system. From the calorimetrically measured divergence of the source, the transport efficiency of beam from the source through the injection window is calculated as given in Fig. 4[5].

Beam composition of hydrogen ions and impurities is measured by momentum analysis magnet[6]. Figure 5 shows the fraction of proton and molecular ions. Dominant impurities are oxygen and their hydrides. The amount of O^+, OH^+, H_2O^+ and H_3O^+ are about 0.4%, 0.4%, 1.3% and 0.1% of the drain current, respectively.

Ion source is magnetically shielded against a stray field such as poloidal field due to the plasma current. At first, the short coaxial shield is used to surround the accel gap. The drain current, in this case, is drastically disturbed as shown in Fig. 6. Therefore, the long mild steel shield is piled up to the shorter shield as illustrated in Fig. 7, where the whole of the source is covered except over the zwischen region. As a result, good shield is attained.

The neutralizer is of 60 cm length and 8 cm diameter, and has conductance of 390 ℓ/sec for hydrogen gas. Working hydrogen gas is

supplied by a pulsed gas feed system[7]. Gas flow rate into each source was of 4 Torr ℓ/sec during 0.2 sec in the heating experiment. Resultant gas thickness in the neutralizer is 0.3 Torr cm, whitch is sufficient for equilibrium neutralization.

The charged beam remaining after neutralizer is deflected by the toroidal magnetic field and the poloidal field due to plasma current in the drift tube region. In order to trap the deflected beam, the powerful sublimer of titanium is installed, by which the evaporation film grows in a rate of 90 Å/ min.

To prevent the direct hit of neutral beam, the drift tube is tapered and of 87 mm x 54 mm entrance, 120 mm x 54 mm exit and 55 cm long. The conductance is 410 ℓ/sec. The differential pumping between the neutralizer and drift tube is performed by two turbomolecular pumps of 1000 ℓ/sec each and a bulk getter pump of 2000 ℓ/sec. A diagram of pump system and the throughput characteristics of pumps are shown in Figs. 8 and 9. The manifold is about 800 ℓ and functions an expansion chamber. By this pumping, the reionization of energetic neutrals in the drift tube is reduced below 18%, and the ion source flashing is carried at an interval of about 5 sec for reduction of impurities in the beam.

The power supply is composed of a set of acceleration and deceleration supply and two sets of arc, filament and magnet coil supplies. Hence the independent operation of two ion sources is permitted. The skeleton is shown in Fig. 10. The accel-decel power supply is designed to cope with the breakdown between extraction gaps. Both voltages are regulated by the series tubes, EIMAC Y-676 for acceleration and NEC 8T43R for deceleration. The tubes also serve to turn off the applied voltage in the case of breakdowns, and are switched on after the breakdown is cleared. EIMAC tube is protected by thyristor switch in the case of misoperation. The turn-off time of the valve systems is less than 0.1 msec.

The capacity of acceleration, deceleration and arc power supplies are 30 kV - 30 A, 5 kV - 4 A and 350 V - 200 A, respectively. These supplies are used up to 10% duty for the pulse duration below 1 sec. The filament and source magnet coil power supplies are of 15 V - 100 A and 15 V - 120 A capacity in DC operation. Table 1 summarizes the nominal values of each power supplies.

To cool the ion source, beam dumpers and other parts, the closed-loop water system of 5 kg/cm^2 pressure and 110 ℓ/min flow is employed. The water is continuously purified through an ion-exchange resin and has high resistivity greater than 1 MΩ-cm. The flow circuit is schematically shown in Fig. 11.

§3 Plasma Heating

The main parameters of JFT-2 tokamak device are a major radius of 90 cm, a round aperture limiter radius of 25 cm, a toroidal magnetic field of 18 kG. By an aluminum shell, a stable equilibrium is maintained below the duration of 150 msec. Before the present heating experiment, an ohmic heating power supply was improved to provide a nearly constant plasma current[8]. The stable and constant current discharges are obtained over the range of $q_a > 4$ and $\bar{n}_e < 2.5 \times 10^{13}$ cm^{-3}. The plasma density is adjusted by the sequence-controlled gas feed at two time intervals for compensating the gas absorption of stainless steel vacuum chamber wall.

Figure 12 shows the typical time behaviour of one-turn loop voltage, plasma current and a central chord averaged density. The density was measured by a 4 mm microwave interferometer. The neutral beam was injected between 40 msec and 100 msec after the initiation of discharge, where the plasma density and current grow up to ionize and trap the energetic beam. The gas to the ion sources was fed regardless of beam on or off. The diagram of time sequence is given in Fig. 13. The gas flow rate from the

injector to the torus in the figure is calculated from the manifold pressure and the conductance of drift tubes. During the pause time of JFT-2, the 60 msec pulse flashing of ion sources was continued every five second in order to reduce the impurity content of the beam.

The central ion temperature was measured by a charge-exchanged neutral analyzer[9] set in the opposit position to the injection port. The analyzer faces the perpendicular direction to the magnetic lines of force. The core electron temperature was derived from soft X-ray detector. Because of perpendicular injection and weak toroidal field, the thickness of target plasma is relatively thin, so that the passing beam without ionization through a plasma is not ignorable and hits the beam dumper in the vacuum chamber. For this reason, the sputtered metal and desorbed impurities were monitored by a visible spectrometer and a soft X-ray detector. The arrangement of these instruments is illustrated in Fig. 14.

The typical time evolution of electron and ion temperature of target plasma is given in Fig. 15, where the discharge conditions are the same as shown in Fig. 12. The temperature is fully raised up to T_e = 1 keV and T_i =0.25 keV at 50 msec. In this case, the electron conductivity temperature was 0.2 keV for an effective charge(Z_{eff}) of unity. On account of this, Z_{eff} is estimated arround five supposing a parabolic profile on electron temperature. To obtain a precise Z_{eff} value, the measurement is planned on the enhancement factor of Bremsstrahlung radiation in a comming experiment. The dependence of ion temperature(T_i) and neutral hydrogen density(n_0) on the electron density are shown in Fig. 16, where the discharges indicated by solid circles are made in a different week from those indicated by crosses. In the ion temperature figure, the solid line represent Artsimovich's scaling law, and the cross points under the line correspond to larger neutral density. The electron temperature hardly depends on plasma density.

Injection heating was done under the conditions of ion source drain current of 6 A at 30 kV and 8 A at 25 kV extraction. The injection did not almost disturb the macroscopic plasma parameters. No effects on the loop voltage and plasma current could be detected. The line radiation of Mo-L_α increases less than a few per cent. The change of visible lines from carbon and oxygen cannot be detected either. The electron density was found to increase by several per cent, roughly corresponding to trapped beam current. To estimate an amount of molybdenum, we assume that all the beam hits the wall and that the sputtered molybdenum is accumulated in a plasma. The number is calculated to be 4.8×10^{15} nuclei for sputtering yield of 0.4%.

The rise in ion temperature is derived by plotting the ratio of the charge exchanged neutral counts during the injection to those in the absence of injection(Fig. 17). In the range of thermal energy($E<7T_i$)[10], above ratio should be proportional to $\exp(E\ \delta T_i/T_i^2)$. The ion temperature increment derived from the tangent in this manner is given in Fig. 18. Figure 19 shows the perpendicular energy spectrum of suprathermal protons for the following parameters; B_t = 18 kG, I_p = 160 kA, V_{loop} = 1.6 V, $\bar{n}_e = 1.1 \times 10^{13}$ cm^{-3} and T_i = 0.29 keV. In the figure, F is proton velocity distribution function.

Energetic ion spectrum is governed by many parameters of a target plasma, especially by the location of a loss cone in a velocity space and by the ratio of charge exchange rate(ν_{cx}) to slowing down rate(ν_s). In the present experiment, however, above two quantities are not clear, because of the absence of a plasma current profile measurement and of uncertainty of proton-electron ratio, whitch will be examined in a comming experiment. Conversely, we try to estimate the quantities based on the classical Fokker-Planck equation. Figure 20 gives the loss cone of the particles passing a point of r=0. The shape of the cone at different

radial position is roughly similar, except for the reduction of the energy scale. On account of this, the energy scale of loss cone is appraised in such a way that the calculated ratio of peak value of the full energy part of energy spectrum to that of the half energy part agrees with the observed ratio. The energy scale obtained is identical to that for uniform plasma current. Then, by fitting the spectrum, the value of ν_{cx}/ν_s is determined to be 4 - 8, namely, $n_0/n_e = (2.2 - 4.5) \times 10^{-5}$. The calculated spectra are given in Fig. 19, where the dotted line for $\nu_{cx}/\nu_s = 4$ and the solid line for $\nu_{cx}/\nu_s = 8$. In the calculation, the employed plasma parameters are $n_e = 1.5 \times 10^{13}$ cm^{-3}, $T_e = 1.0$ keV, $T_i = 0.3$ keV, $Z_{eff} = 5$, $I_p = 160$ kA and $V_{loop} = 1.6$ V.

The fraction of the beam power transferred to the ions(G_i) can be derived from the energetic ion spectrum,

$$G_i = - \int d^3v \; C_{bi}(F) \; E/S_0 \; E_0$$

where C_{bi} is the classical collision term between energetic beam and thermal ions, S_0 the particle source, and E_0 the injection energy. Using the above-derived spectra, the values of G_i for full, half and one-third energy part are calculated to be 7.3%, 25.4% and 45.0% for $\nu_{cx}/\nu_s = 4$ and 4.2%, 16.4% and 32.2% for $\nu_{cx}/\nu_s = 8$, respectively. Accordingly the power flow is summarized as given in Tab. 2, where the effective ionization cross-section of neutral beam is employed to be an energy independent value of 1.0×10^{-15} cm^2, reflecting an impurity impact ionization. In addition, the expected $\delta T_i/T_i$ value is calculated by applying the scaling law of $\delta T_i/T_i = 2 P_i^{NBI}/3 P_{ei}$. Comparing the experimental value of ion temperature rise with the expected value, the contradiction is not seen.

The authors are grateful to Messrs. S. Kunieda and N. Toyoshima, and the members of facility operation and engineering section for operation of JFT-2 device. They are also indebted to Dr. T. Shoji and Mr. T. Kawakami

for aid in data-processing, and to Dr. S. Mori for his support and encouragement.

REFERENCES

[1] TFR group; Paper IAEA-CN-35/A4-2 in 6 th International Conference on Plasma Physics and Controlled Nuclear Fusion Research, Berchtesgaden, 1976.

[2] L. A. Berry et al; ibid, IAEA-CN-35/A4-1.

[3] R. C. Davis et al; ORNL-TM 4675(1974).

[4] L. D. Stewart et al; Rev. Sci. Instr. 46(1975)1193.

[5] Y. Ohara et al; JAERI-M 6438(1976).

[6] T. Shibata et al; JAERI-M 6990(1977).

[7] S. Tanaka and T. Shibata; JAERI-M 6778(1976).

[8] M. Maeno, Y. Matsuzaki and N. Fujisawa; JAERI-M 6762(1976).

[9] H. Takeuchi et al; JJAP 16(1977)139.

[10] J. G. Cordey; Paper IAEA-CN-33/A16-1 in 5 th International Conference on Plasma Physics and Controlled Nuclear Fusion Research, Tokyo, 1974.

FIGURE CAPTIONS

Fig. 1 Neutral beam injector. Injection angle is changed by moving the injector on a rail.

Fig. 2 Cross-section of duoPIGatron ion source.

Fig. 3 Extraction electrode system. The electrode in contact with source plasma is recessed as given in upper figure. The bended angle of a beamlet($\Delta\theta$) experimentally obtained is equal to 18.4 $\Delta r/d$ degrees. Lower figure shows the whole aspect of electrodes: R_0 = 3.9 cm, R_1 = 1.49 m, R_2 = 67 cm, d(0) = 4.7 mm, $d(R_0)$ = 6.35 mm, Δh_1= 0.51 mm and Δh_2= 1.14 mm.

Fig. 4 Transport efficiency of energetic beam from the source through the injection window.

Fig. 5 Fraction of proton and molecular ions from ion source.

Fig. 6 Shorter magnetic shield for ion source and shield effect. The upper and lower oscillogram traces give the drain current for I_p= 0 and 170 kA, respectively. The scale of vertical axis is 1 A/div.

Fig. 7 Piled up shield and shield effect. The upper and lower oscillogram traces give the drain current for I_p= 0 and 170 kA, respectively. The scale of vertical axis is 1 A/div.

Fig. 8 Diagram of pumping system: IS-ion source,TMP-turbomolecular pump, PMB-mechanical booster pump, RP-rotary pump, SORB-AC - getter pump, GGT-titanium sublimer, PST-sputter ion pump.

Fig. 9 Throughput versus inlet hydrogen pressure for turbomolecular pump and getter pump.

Fig. 10 Skeleton of power supply.

Fig. 11 Flow circuit of cooling system: CT-cooling tower, WT-water tank, IE-ion exchange resin, P-pressure gauge, T-thermometer.

Fig. 12 One turn loop voltage,plasma current and central chord-averaged electron density of a typical discharge. One fringe corresponds to the thickness of 5.2×10^{13} cm^{-2}.

Fig. 13 Time sequence diagram of gas feed and beam pulse.

Fig. 14 JFT-2 device and arrangement of instruments.

Fig. 15 Time evolution of electron and ion temperature.

Fig. 16 Dependence of ion temperature and neutral hydrogen density on the electron density for the discharges of I_p=160 kA and B_t=18 kG. The solid circles and crosses indicate the target plasma for 30 kV-6 A and 25 kV-8 A injection, respectively.

Fig. 17 Ratio of the charge exchanged neutral counts during the injection (F_{ON}) to that in the absence of injection(F_{OFF}) for $\bar{n}_e = 1.1 \times 10^{13}$ cm^{-3} discharge.

Fig. 18 Ion temperature rise versus electron density. The solid circles and crosses indicate 30 kV-6 A and 25 kV-8 A injection, respectively.

Fig. 19 Ion energy spectrum during the injection for $\bar{n}_e = 1.1 \times 10^{13}$ cm^{-3}, I_p= 160 kA and B_t= 18 kG discharge. The lines indicate theoretically derived spectra for ν_{cx}/ν_s= 4(dotted line) and ν_{cx}/ν_s= 8(solid line). The plasma parameters used are $n_e = 1.5 \times 10^{13}$ cm^{-3}, T_e = 1 keV, T_i = 0.3 keV, Z_{eff} = 5 and V_{loop}= 1.6 V.

Fig. 20 Loss cone of the particles passing a point of r=0. In the horizontal axis, B_θ and B_a are the poloidal magnetic field at any radial position and at a plasma surface, respectively.

Tab. 1 Capacity of power supply

	ACCELERATION	DECELERATION	ARC	FILAMENT	MAGNET COIL
CAPACITY	30 kV - 30 A one set	5 kV - 4 A one set	350 V - 200 A two sets	15 V - 100 A two sets	15 V - 120 A two sets
OPERATION	PULSE*	PULSE*	PULSE*	DC	DC
REGULATION	± 1 % EIMAC Y 676	± 5 % NEC 8T43R	UNREGULATED**	UNREGULATED**	UNREGULATED**
CURRENT RISE TIME	1 msec	1 msec	0.1 msec	———	———

*) The pulse width and duty are less than 1 sec and 10 %, respectively.

**) The ripple is less than 1 %.

Tab. 2 Calculated power flow and ion temperature rise.

ION SOURCE OUTPUT 30 kV - 6 A	H^+ 2.4 A 1.0 A	H_2^+ 0.96 A 0.48 A	H_3^+ 0.64 A 0.52 A	 4 A 2 A
NEUTRAL BEAM CURRENT THROUGH THE PORT	0.93 A	1.02 A	1.24 A	3.19 A
NEUTRAL POWER TRANSFERRED TO PLASMA	11.74kW	6.43kW	5.27kW	23.44kW
TRANSFERRED POWER TO IONS	0.86kW* 0.49kW**	1.63kW* 1.05kW**	2.37kW* 1.70kW**	4.86kW* 3.24kW**
TRANSFERRED POWER FROM ELECTRONS TO IONS				30.8 kW
EXPECTED $\delta T_i/T_i$			7 %** -	10.5 %*

*) $\nu_{cx}/\nu_s = 4$
**) $\nu_{cx}/\nu_s = 8$

1 ION SOURCE
2 NEUTRALIZER
3 MAGNETIC SHIELD
4 FLASHING TARGET
5 DRIFT TUBE
6 TITANIUM SUBLIMER
7 MOLYBDENUM TARGET
8 TITANIUM GETTER
9 TURBOMOLECULAR PUMP
10 VACUUM CHAMBER
11 TOROIDAL COIL
12 RAIL

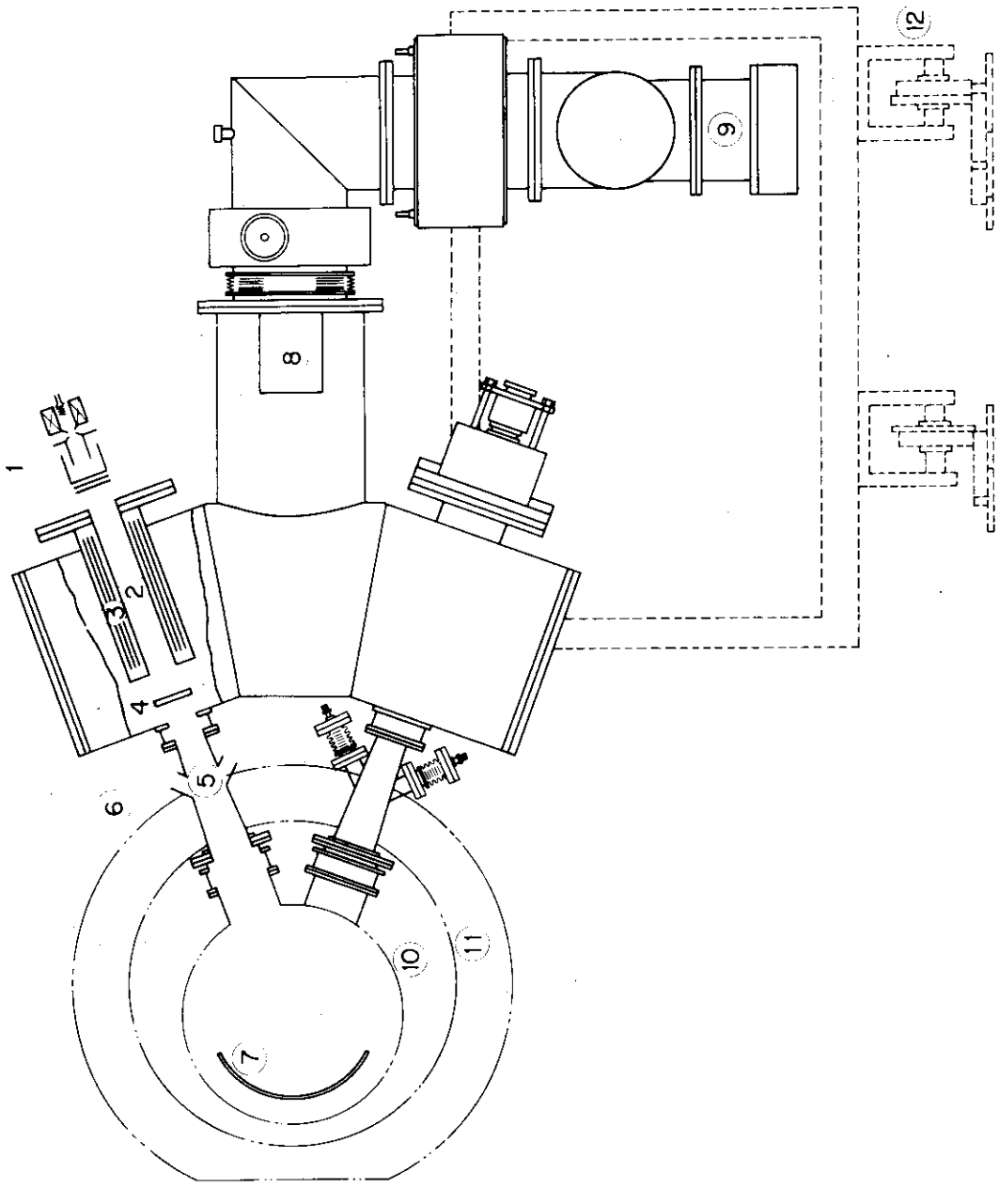

Fig. 1

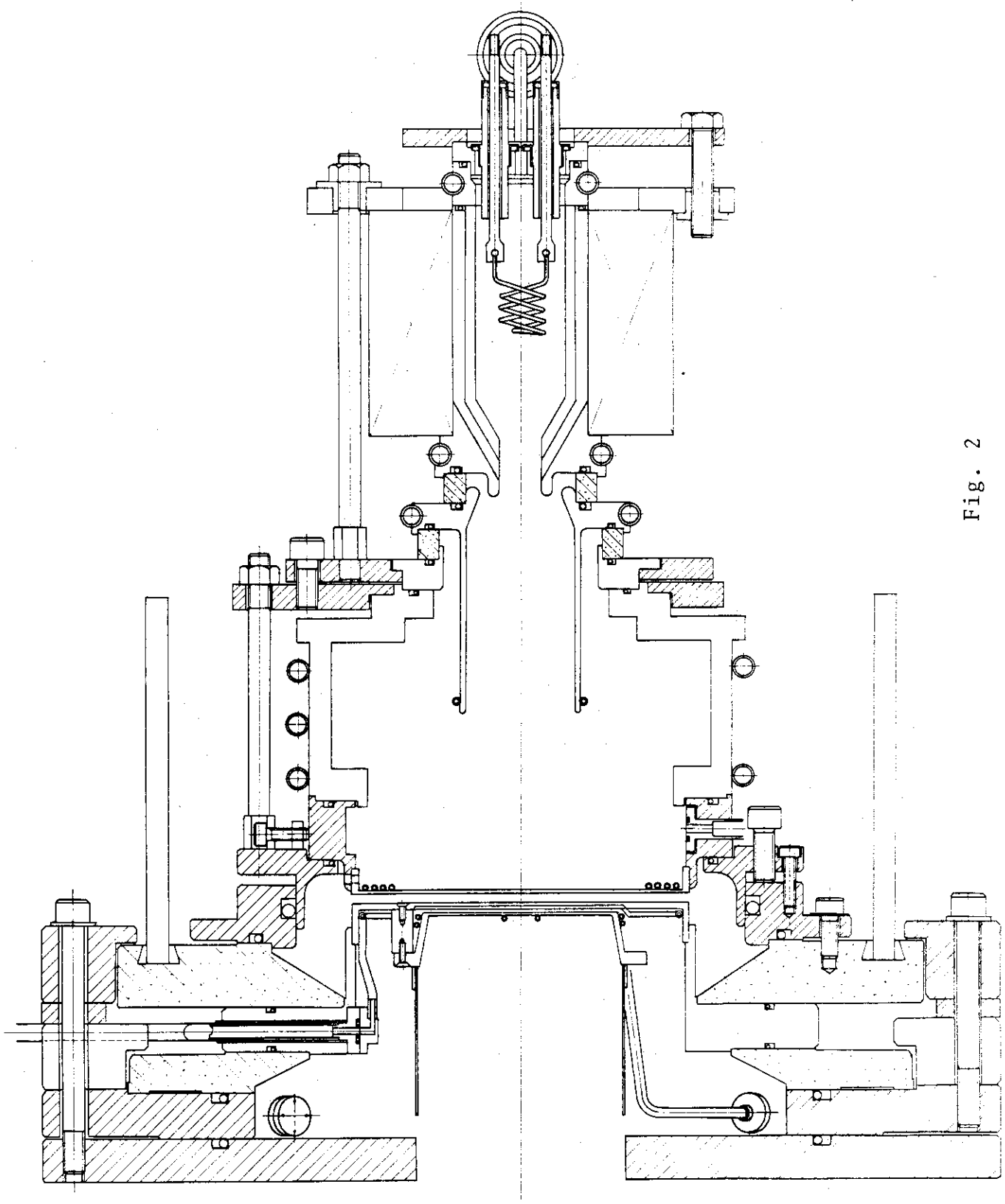

Fig. 2

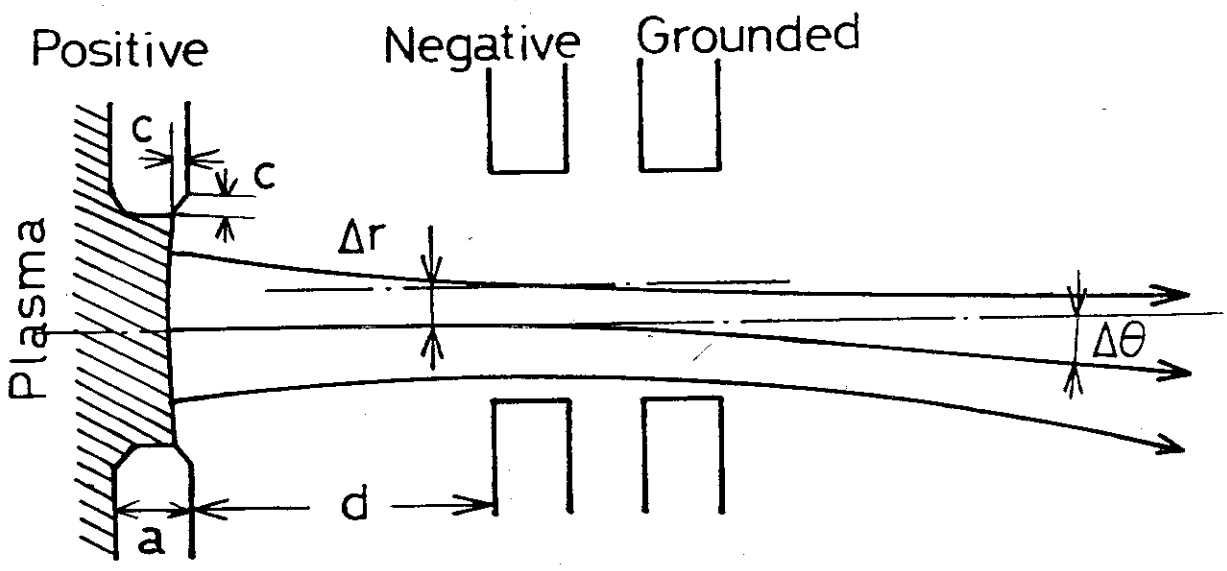
Positive
Negative
Grounded
c
c
Plasma
Δr
Δθ
d
a

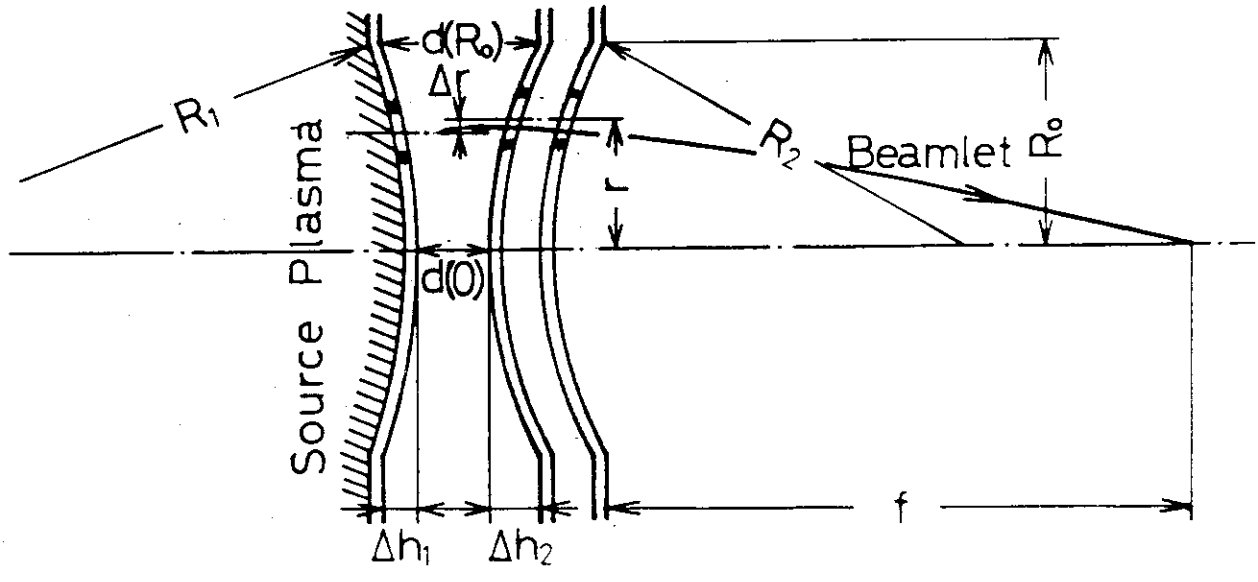
d(R₀)
Δr
R₁
R₂
Beamlet
R°
L
Source Plasma
d(0)
f
Δh₁
Δh₂

Fig. 3

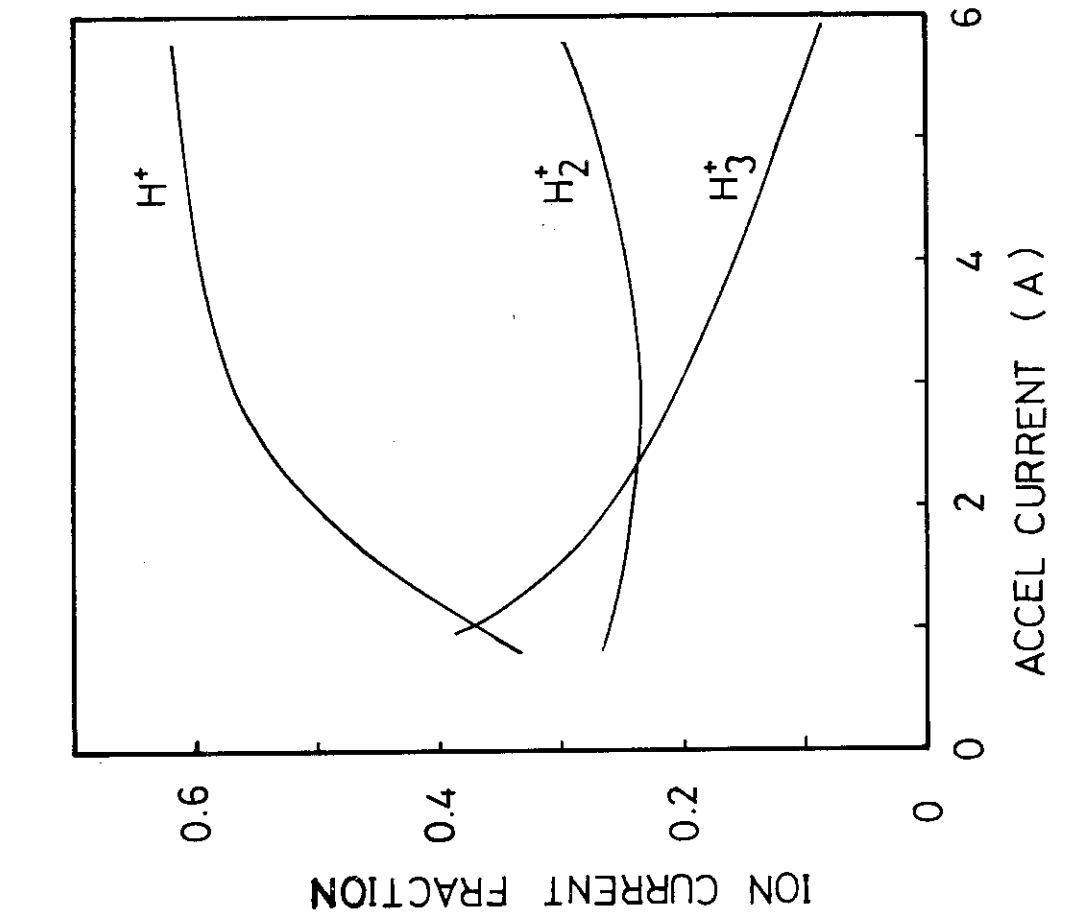
H+
H+2
H+3
ION CURRENT FRACTION
0.6
0.4
0.2
0
0
2
4
6
ACCEL CURRENT (A)

Fig. 5

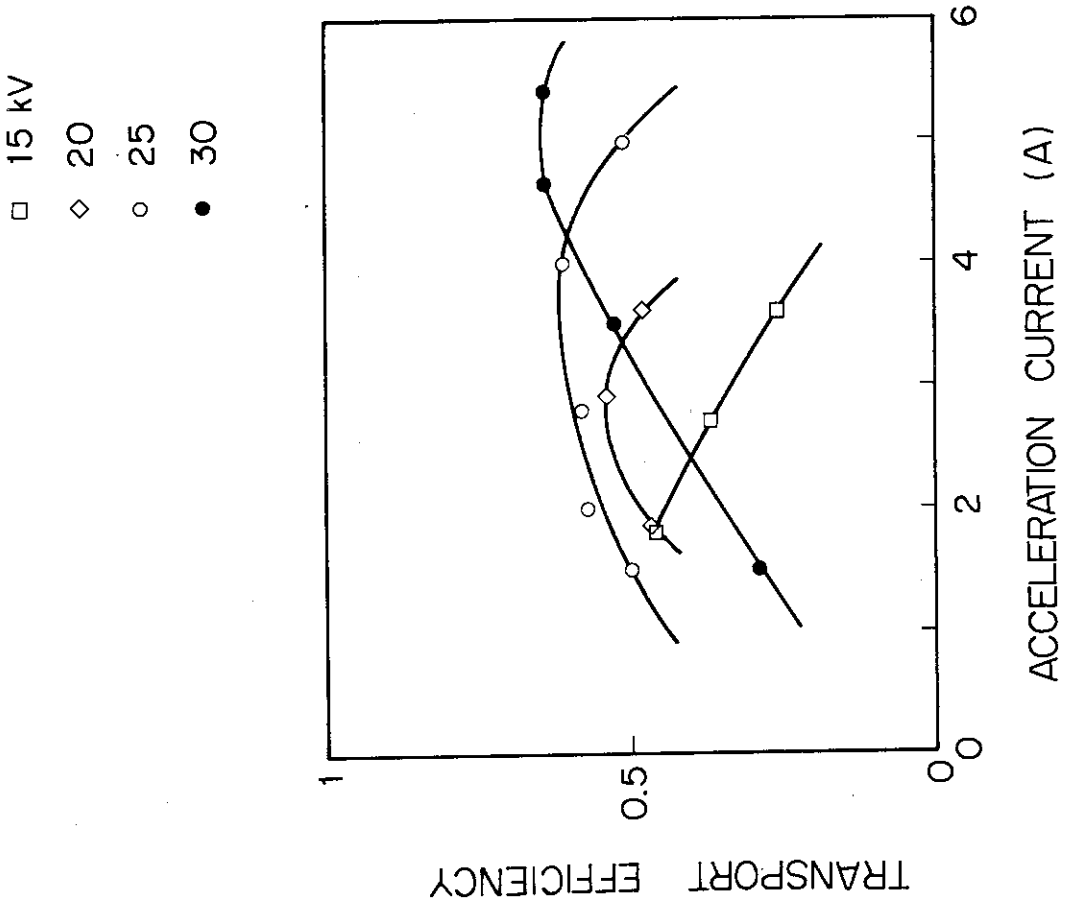
□ 15 kV
◇ 20
○ 25
● 30
TRANSPORT EFFICIENCY
1
0.5
0
0
2
4
6
ACCELERATION CURRENT (A)

Fig. 4

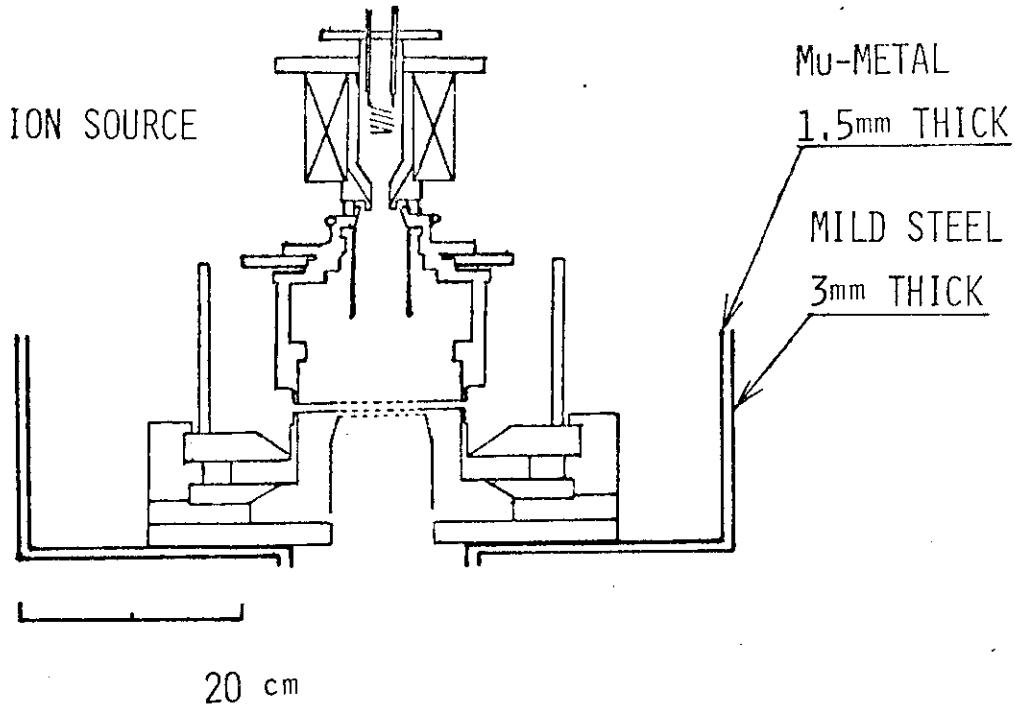
ION SOURCE
Mu-METAL
1.5mm THICK
MILD STEEL
3mm THICK
20 cm

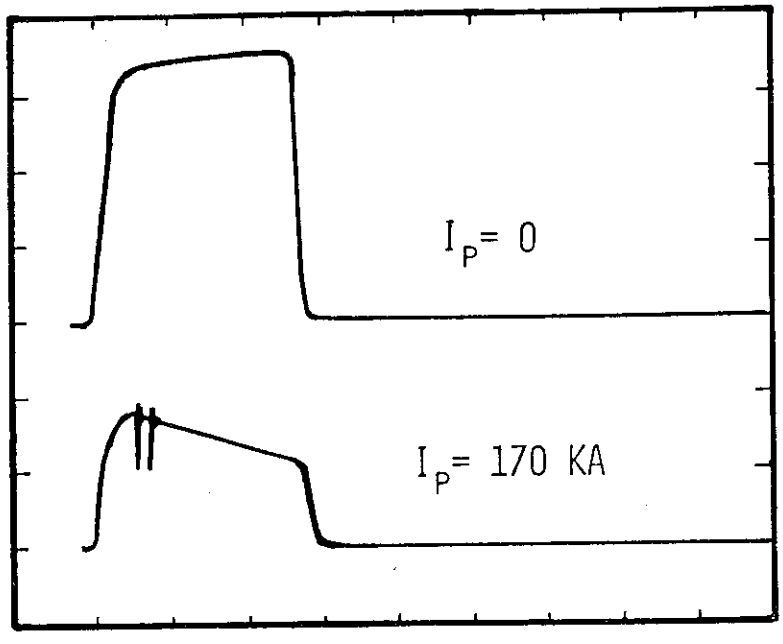
I_P= 0
I_P= 170 KA

Fig. 6

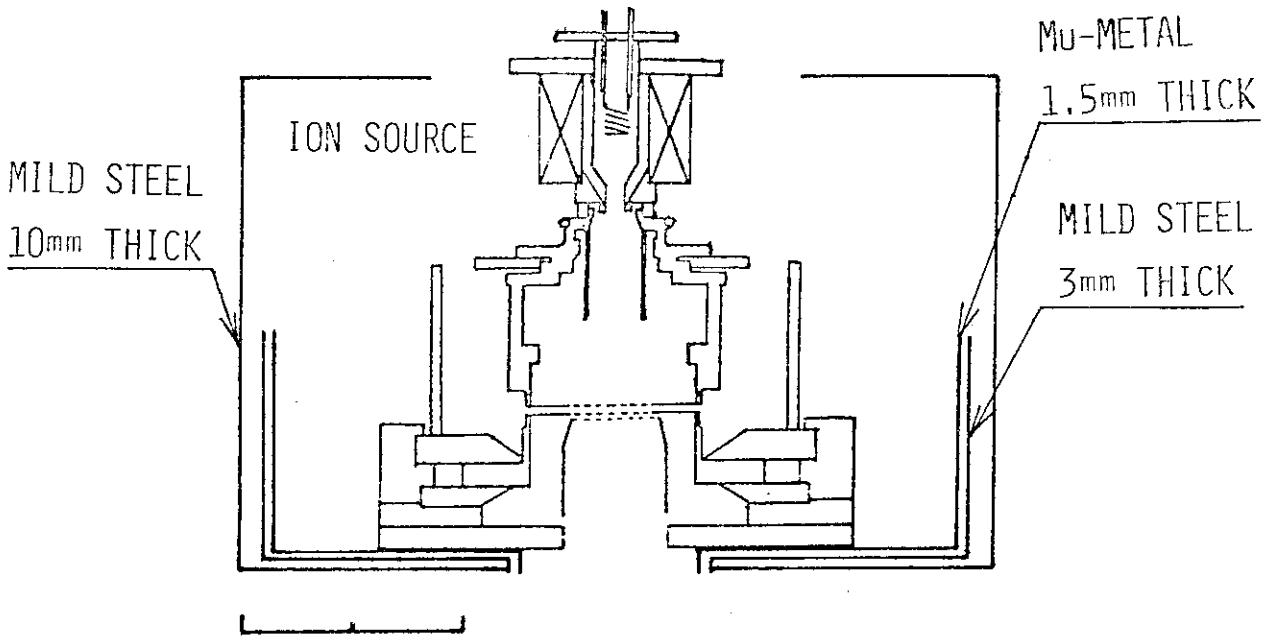
Mu-METAL
1.5mm THICK
ION SOURCE
MILD STEEL
10mm THICK
MILD STEEL
3mm THICK
20 cm

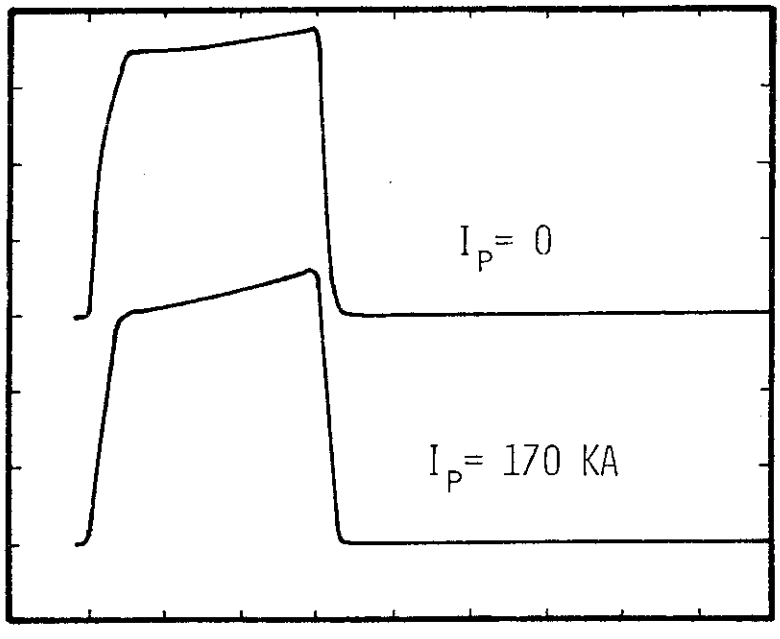
I_P= 0
I_P= 170 KA

Fig. 7

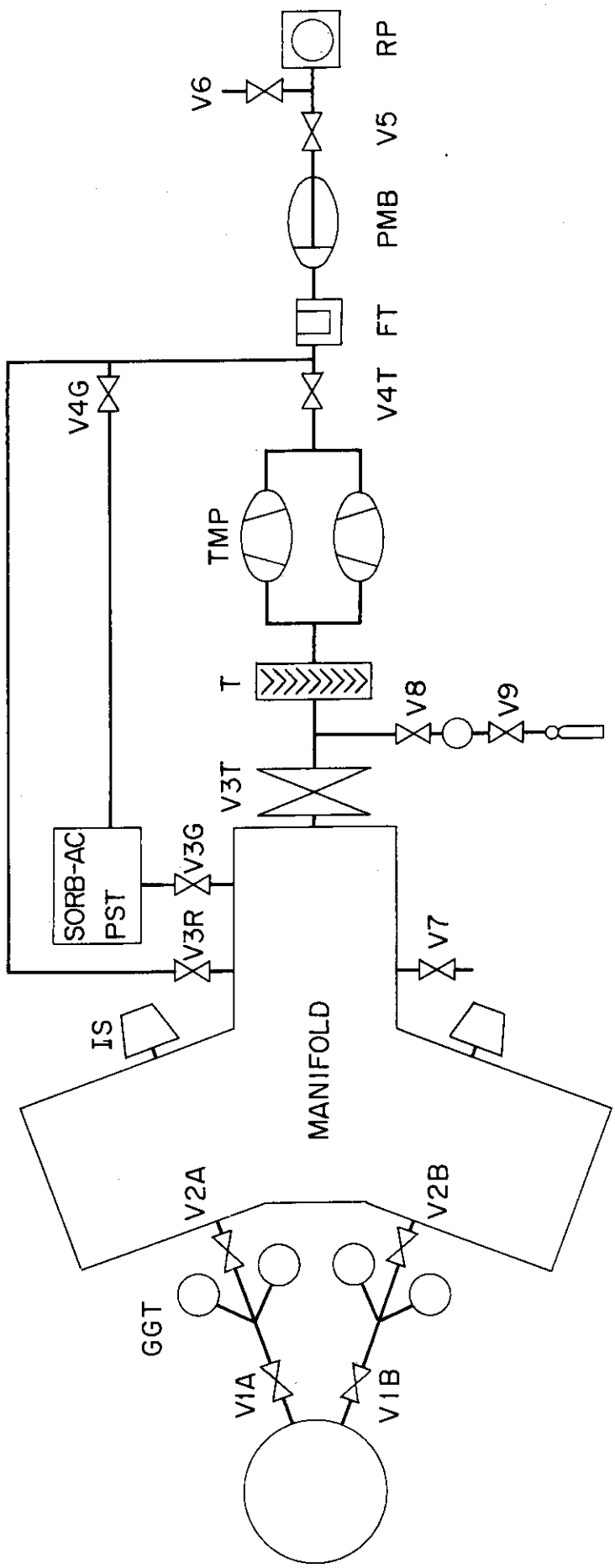
RP
V6
V5
PMB
FT
V4T
V4G
TMP
T
V8
V9
V3T
V3G
SORB-AC
PST
V3R
V7
IS
MANIFOLD
V2A
V2B
GGT
V1A
V1B

Fig. 8

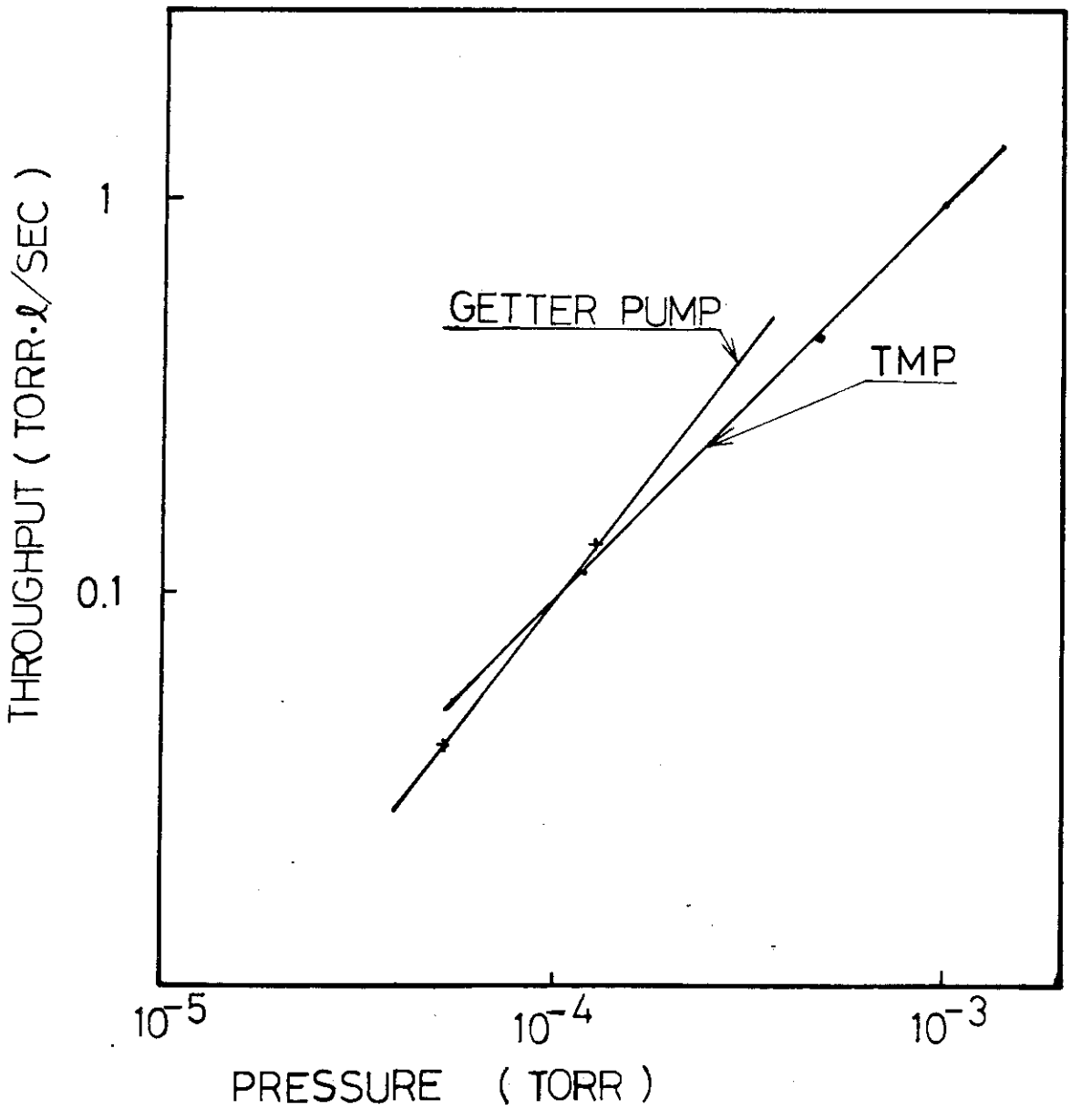
THROUGHPUT (TORR·ℓ/SEC)
1
0.1
GETTER PUMP
TMP
10⁻⁵
10⁻⁴
10⁻³
PRESSURE (TORR)

Fig. 9

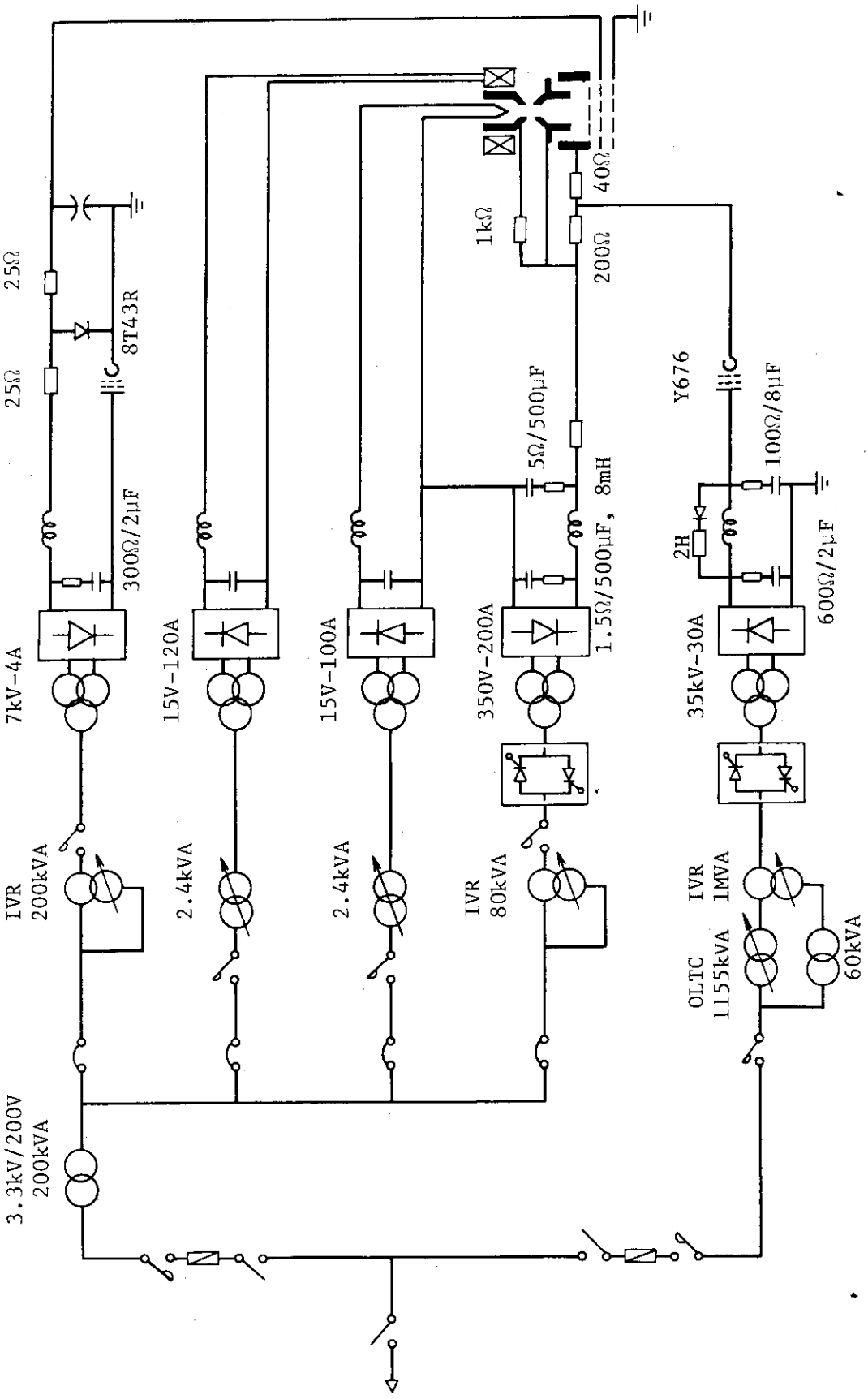
3.3kV/200V
200kVA
IVR
200kVA
7kV-4A
25Ω
25Ω
8T43R
300Ω/2μF
2.4kVA
15V-120A
2.4kVA
15V-100A
IVR
80kVA
350V-200A
5Ω/500μF
1.5Ω/500μF, 8mH
1kΩ
200Ω
40Ω
OLTC
1155kVA
IVR
1MVA
60kVA
35kV-30A
Y676
2H
100Ω/8μF
600Ω/2μF

Fig. 10

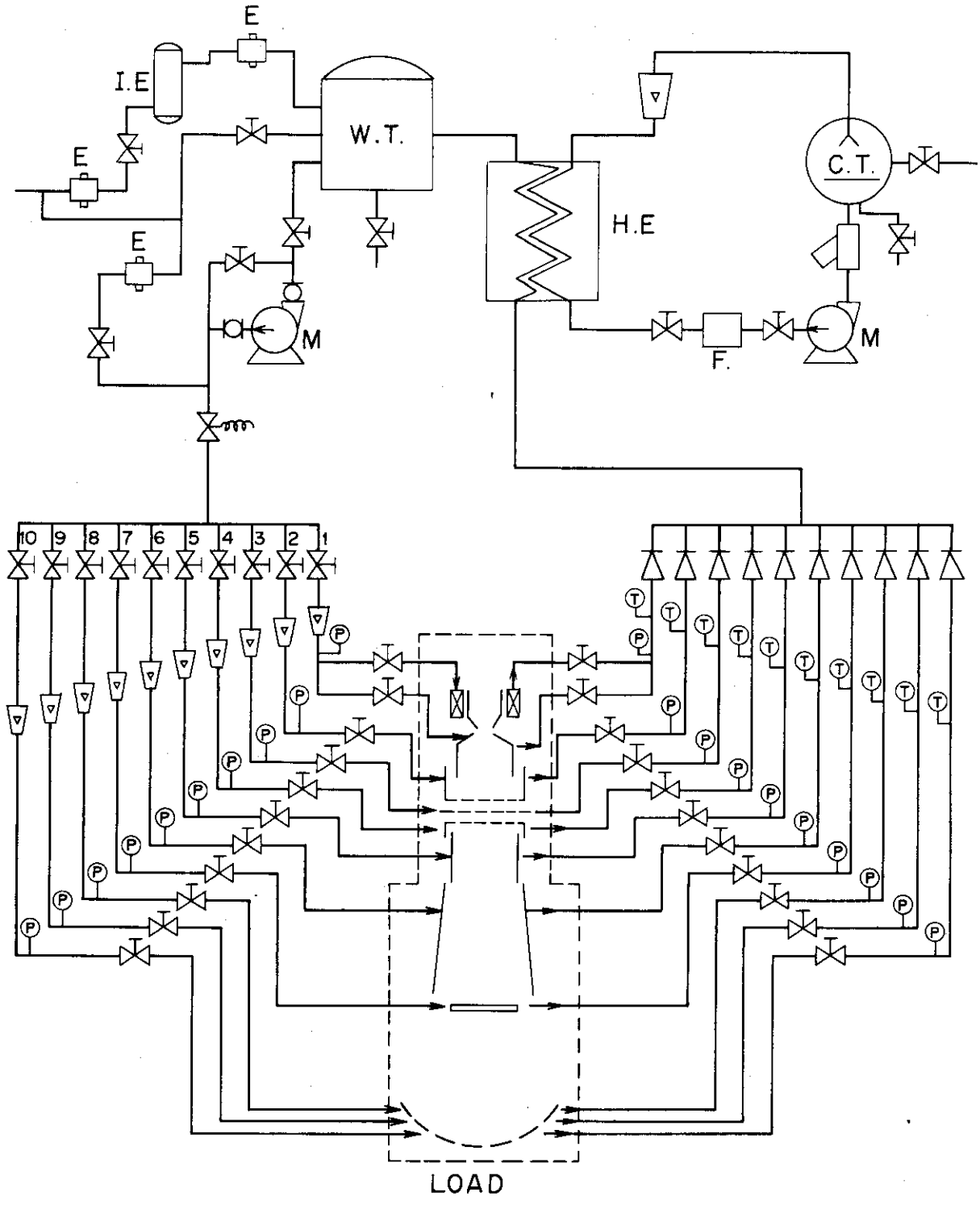

Fig. 11

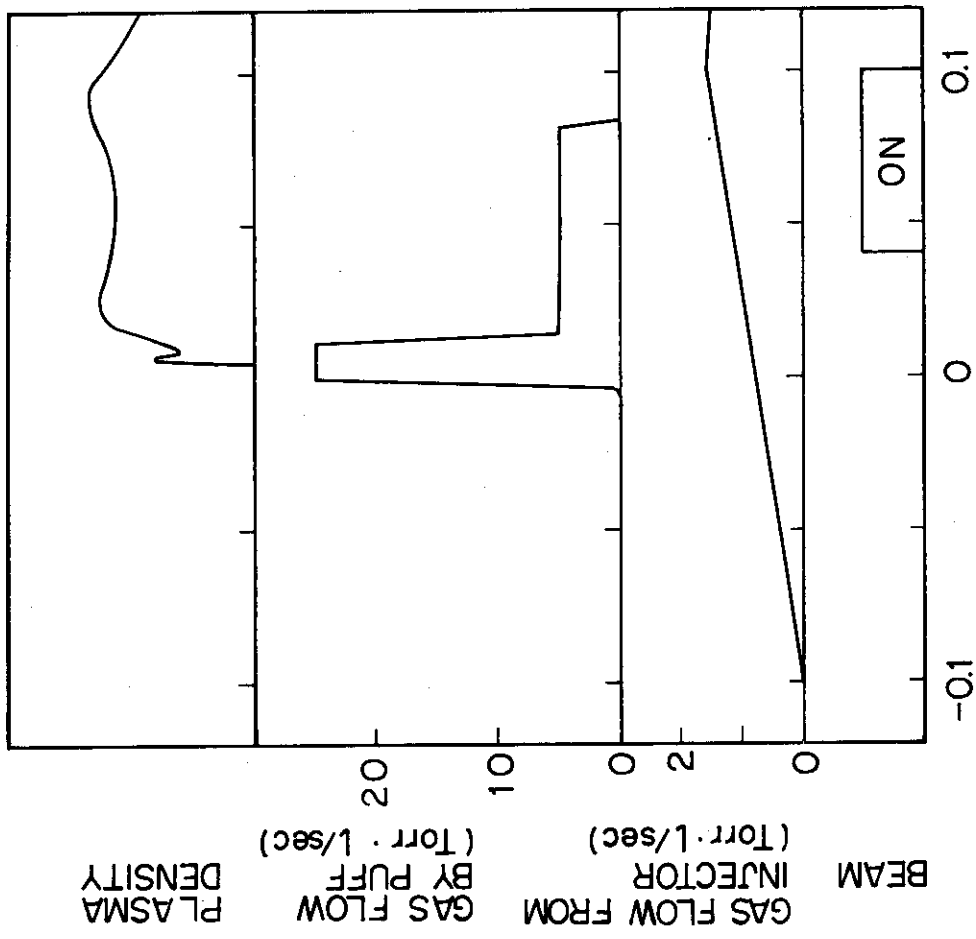
BEAM
GAS FLOW FROM INJECTOR (Torr·L/sec)
GAS FLOW BY PUFF (Torr · L/sec)
PLASMA DENSITY
ON
0
2
0
10
20
-0.1
0
0.1
TIME (sec)

Fig. 13

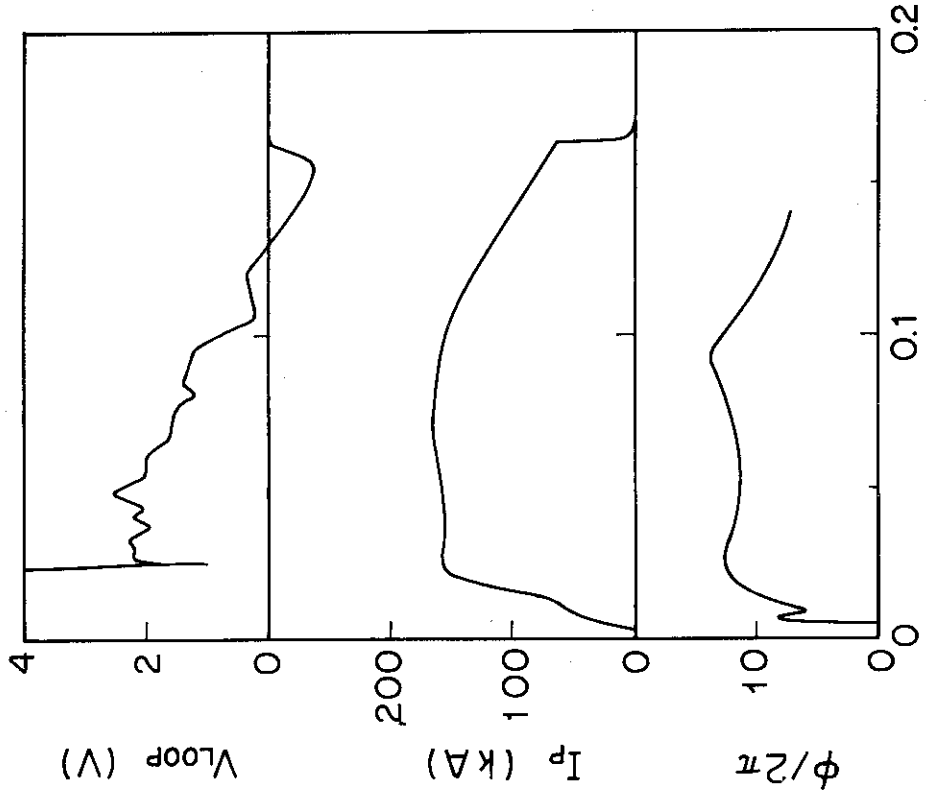
$\phi/2\pi$
I_p (kA)
V_{LOOP} (V)
0
10
0
100
200
0
2
4
0
0.1
0.2
TIME (sec)

Fig. 12

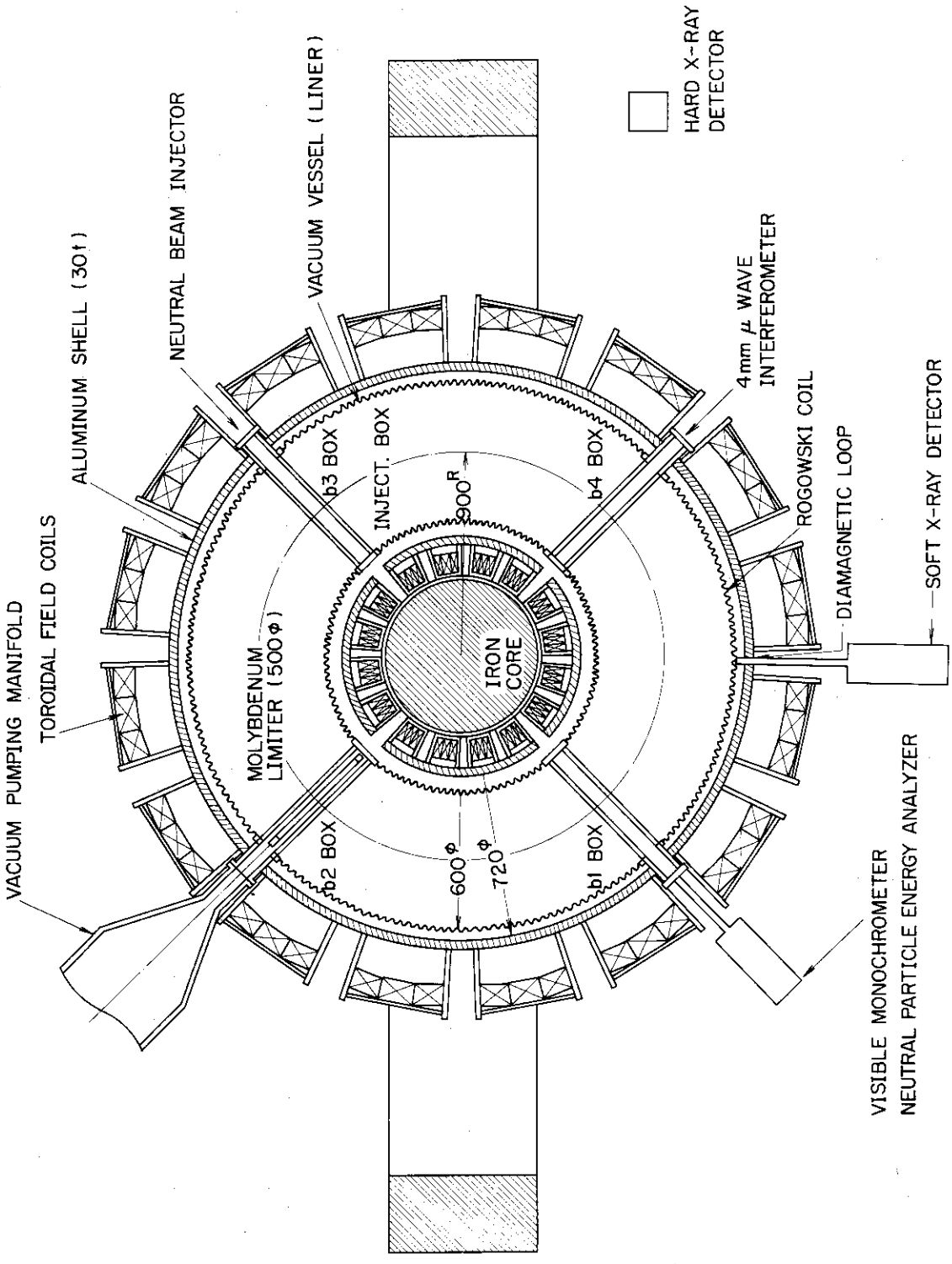
VACUUM PUMPING MANIFOLD
TOROIDAL FIELD COILS
ALUMINUM SHELL (30t)
NEUTRAL BEAM INJECTOR
VACUUM VESSEL (LINER)
HARD X-RAY DETECTOR
4mm μ WAVE INTERFEROMETER
ROGOWSKI COIL
DIAMAGNETIC LOOP
SOFT X-RAY DETECTOR
VISIBLE MONOCHROMETER
NEUTRAL PARTICLE ENERGY ANALYZER
MOLYBDENUM LIMITER (500Φ)
IRON CORE
INJECT. BOX
b1 BOX
b2 BOX
b3 BOX
b4 BOX
900R
600Φ
720Φ

Fig. 14

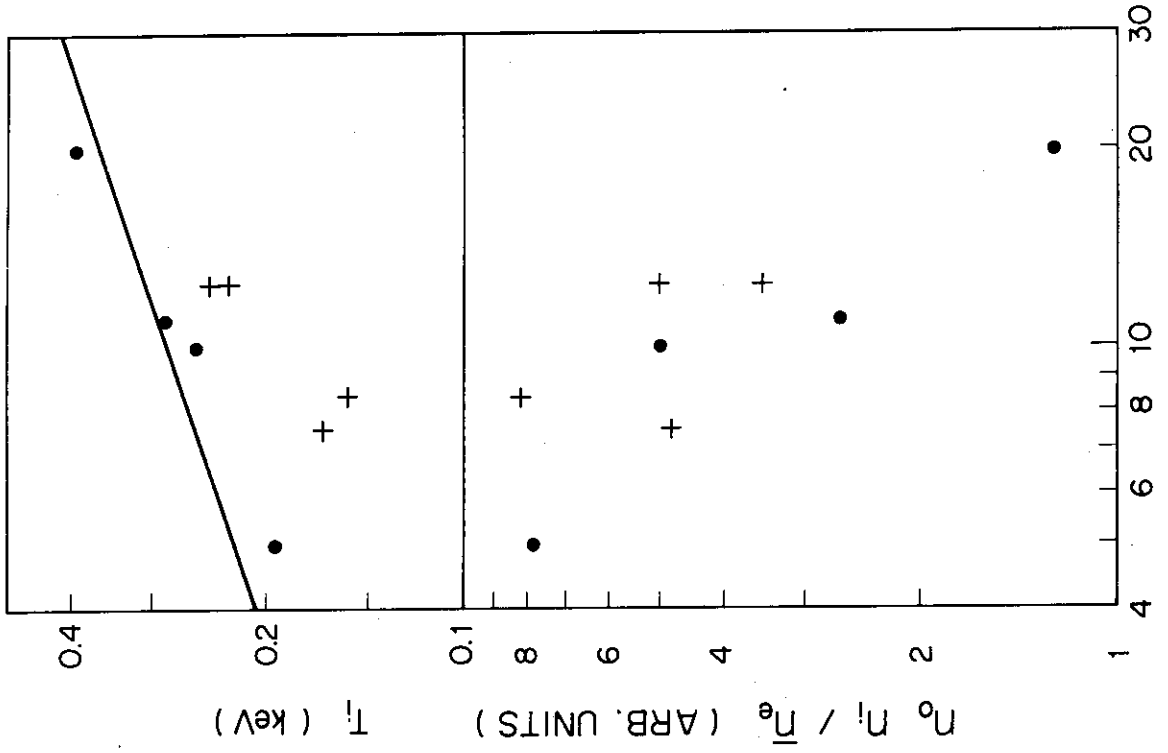
T_i (keV)
n_o n_i / $\bar{n}_e$ (ARB. UNITS)
$\bar{n}_e$ (10^{12} cm^{-3})
0.4
0.2
0.1
8
6
4
2
1
4
6
8
10
20
30

Fig. 16

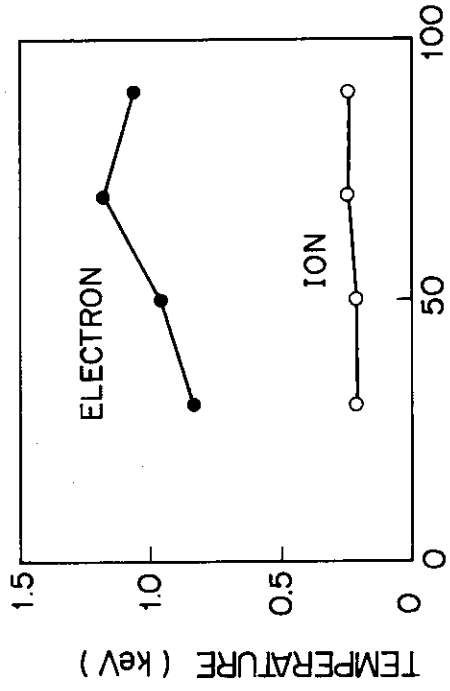
TEMPERATURE (keV)
ELECTRON
ION
TIME (msec)
1.5
1.0
0.5
0
0
50
100

Fig. 15

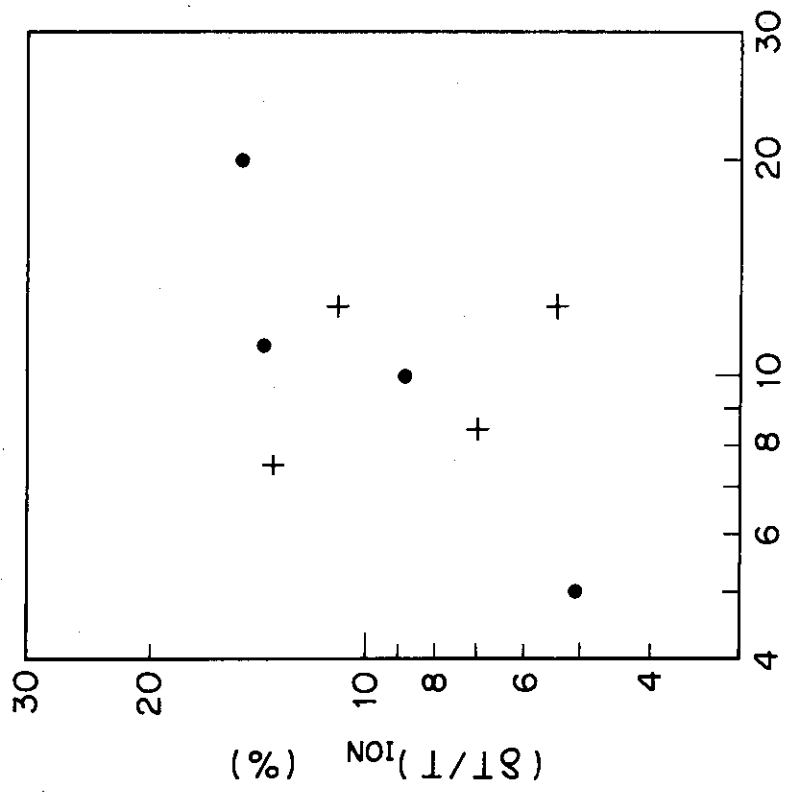
30
20
10
8
6
4
(%)
$(\delta T/T)_{ION}$
30
20
10
8
6
4
$\bar{n}_e$ (10^{12} cm^{-3})

Fig. 18

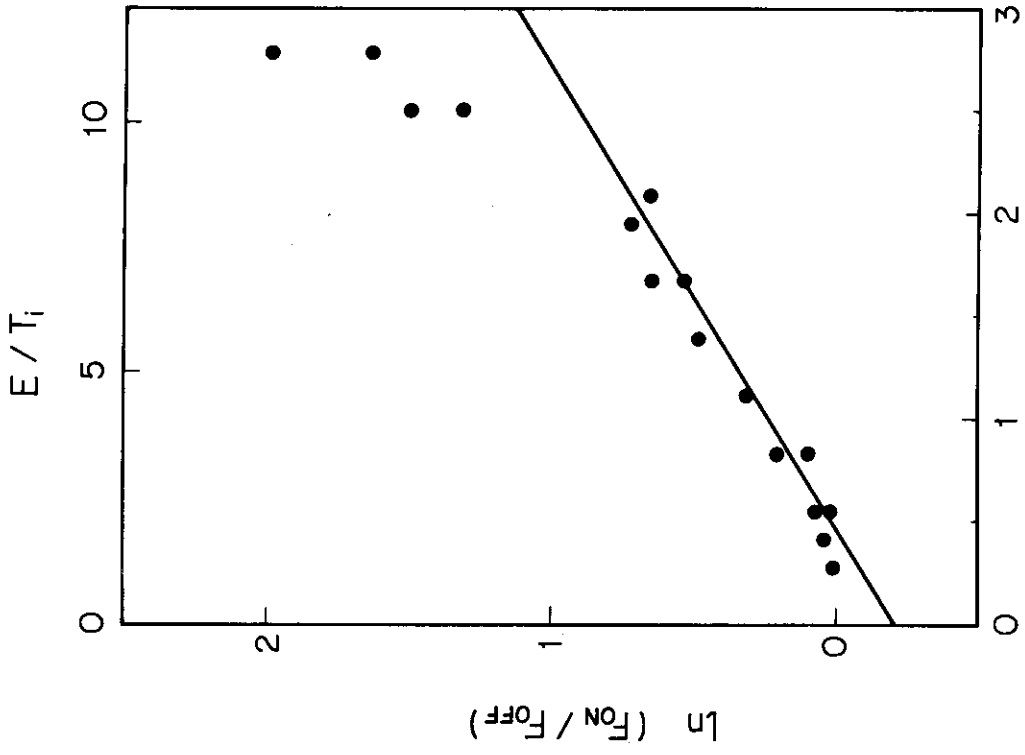
0
5
10
E / T_i
2
1
0
ln (F_{ON} / F_{OFF})
0
1
2
3
ENERGY (keV)

Fig. 17

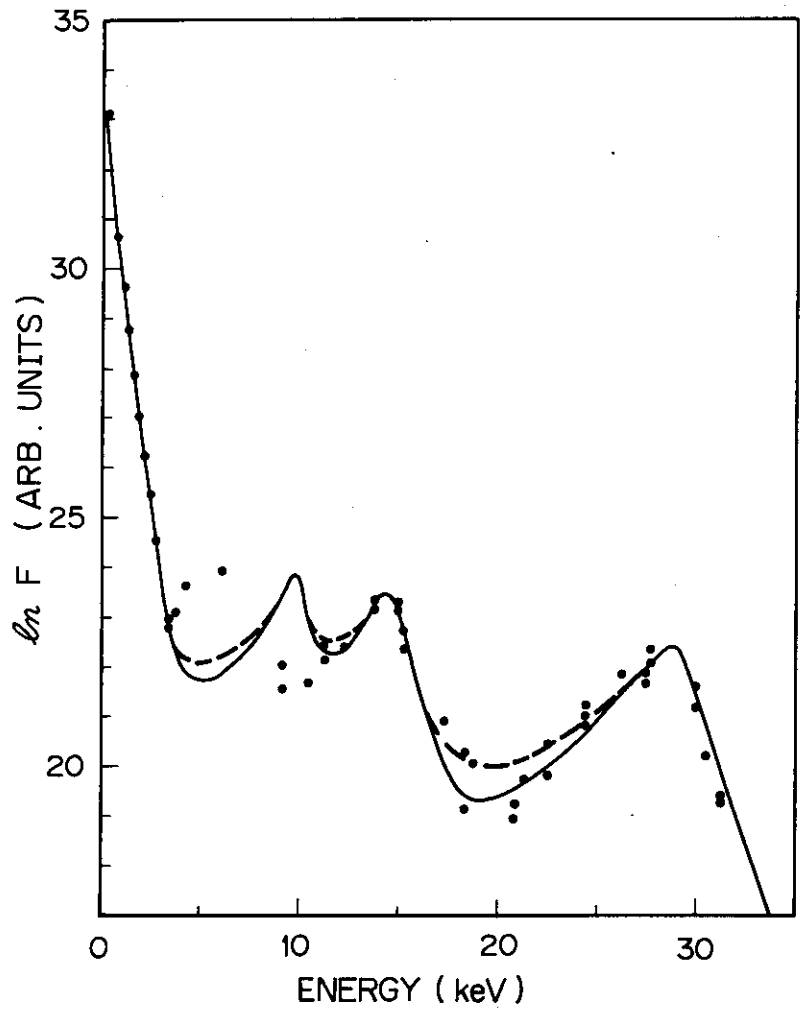
35
30
25
20
ℓn F (ARB. UNITS)
0
10
20
30
ENERGY (keV)

Fig. 19

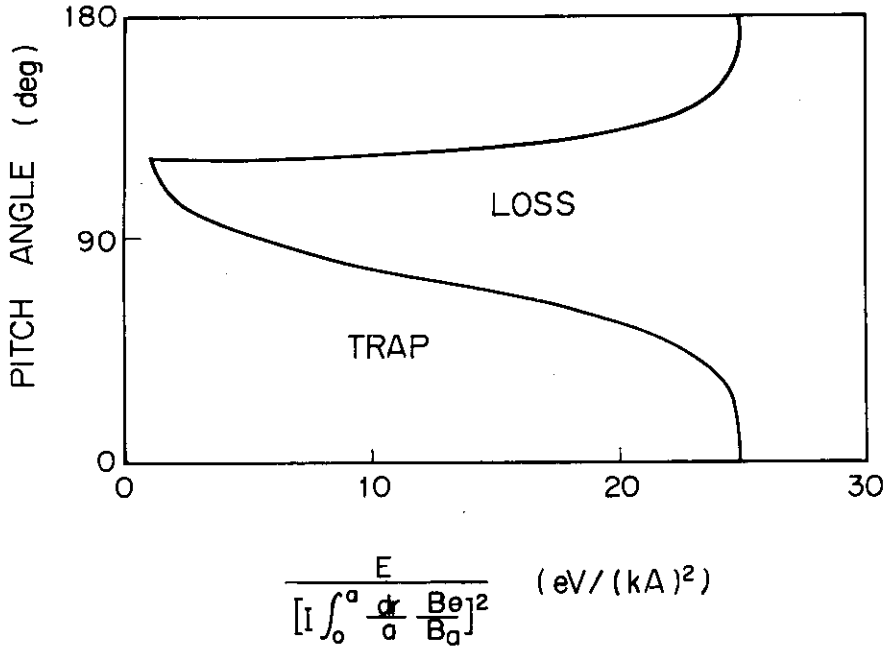
180
90
0
PITCH ANGLE (deg)
LOSS
TRAP
0
10
20
30
$\frac{E}{[I\int_0^a \frac{dr}{a}\frac{B\theta}{B_a}]^2}$ (eV/(kA)²)

Fig. 20